Proceedings of the 2004 IEEE
International Conference on Robotics & Automation
New Orleans, LA • April 2004

Dynamics and Kinematics of Viral Protein Linear Nano-Actuators for Bio-Nano Robotic Systems

A. Dubey[1], G. Sharma[1], C. Mavroidis[1,*], S. M. Tomassone[2], K. Nikitczuk[3], M.L. Yarmush[3]

[1]*Department of Mechanical and Industrial Engineering, Northeastern University, 360 Huntington Ave., Boston MA 02115*

[2]*Department of Chemical and Biochemical Engineering, Rutgers University, 98 Brett Road, NJ 08854*

[3]*Department of Biomedical Engineering, Rutgers University, 98 Brett Road, NJ 08854*

* Author for Correspondence, Tel 617-373-4121, 617-373-2921, Email: mavro@coe.neu.edu

***Abstract*– Dynamic and kinematic analysis is performed to predict and verify the performance of a new nanoscale biomolecular motor: The Viral Protein Linear (VPL) Motor. The motor is based on a conformational change observed in a family of viral envelope proteins when subjected to a changing pH enivronment. The conformational change produces a motion of about 10 nm, making the VPL a basic linear actuator which can be further interfaced with other organic/inorganic nanoscale components such as DNA actuators and carbon nanotubes. The proteins used in the motor are subjected to Molecular Dynamics simulation using the software called CHARMm (Chemistry at Harvard Molecular Mechanics). The results of dynamics are further verified by performing a set of kinematic simulations using direct and inverse kinematics methods.**

Index Terms- Bionano Robotics; Molecular Dynamics; Molecular Kinematics; Molecular Motors.

I. INTRODUCTION

The recent explosion of research in nano-technology, combined with important discoveries in molecular biology have created a new interest in biomolecular machines and robots. The main goal in the field of biomolecular machines is to use various biological elements — whose function at the cellular level creates a motion, force or a signal — as machine components that perform the same function in response to the same biological stimuli but in an artificial setting. In this way proteins and DNA could act as motors, mechanical joints, transmission elements, or sensors. If all these different components were assembled together they could potentially form nanodevices with multiple degrees of freedom, able to apply forces and manipulate objects in the nanoscale world, transfer information from the nano- to the macroscale world and even travel in a nanoscale environment.

Just as conventional macro-machines are used to develop forces and motions to accomplish specific tasks, bio-nano-machines can be used to manipulate nano-objects, to assemble and fabricate other machines or products and to perform maintenance, repair and inspection operations. The advantages in developing bio-nano-machines include: a) energy efficiency due to their intermolecular and interatomic interactions; b) low maintenance needs and high reliability due to the lack of wear and also due to nature's homeostatic mechanisms (self-optimization and self-adaptation); c) low cost of production due their small size and natural existence. Figure 1 shows one such concept of a nano-organism, with its 'feet' made of helical peptides and its body using carbon nanotubes while the power unit is a biomolecular motor. Our goal is that just as conventional macro-machines are used to develop forces and motions to accomplish specific tasks, bio-nano-machines can be used to manipulate nano-objects, to assemble and fabricate other machines or products, to perform maintenance, repair and inspection operations.

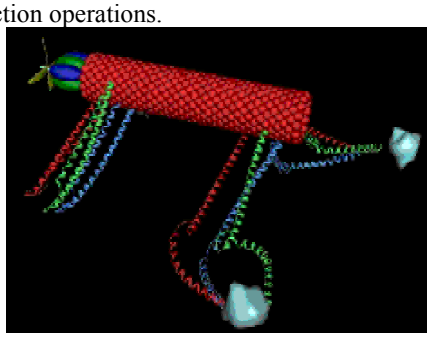

Fig. 1 A vision of a nano-organism: carbon nano-tubes form the main body; peptide limbs can be used for locomotion and object manipulation. A biomolecular motor located at the head can propel the device in various environments.

In this project, we are studying the development of Viral Protein Linear (VPL) nano-motors and their integration as actuators in bio-nano-robotic systems. The project consists of three research phases: 1) Development of concepts for novel bio-nano-motors and devices; 2) Performance of computational studies to develop models and design procedures that will predict and optimize the performance of the proposed bio-nano motors and systems; and 3) Execution of experimental studies to demonstrate the validity of the proposed concepts, models and design methodologies. In this paper we present the current activities and results for the first two phases. More specifically we will present the principle of operation of the VPL motor, the development of dynamic and kinematic models to study their performance and preliminary results obtained from the developed computational tools.

II. BACKGROUND

There is a novel engineering interest in utilizing machines, which have always been an integral part of all life. These motors, which are called *Biomolecular Motors* have attracted a great deal of attention recently because they have high efficiency, they could be self-replicating, hence cheaper in mass usage, and they are readily available in nature. A number of enzymes such as kinesin [1, 2], RNA polymerase [3], myosin [4], dynein [5] and adenosine triphosphate (ATP) synthase [6] function as nanoscale linear, oscillatory or rotary biological motors. Other machines that have been extensively studied include the flagella motors [7] and the rotaxanes [8],

which are an example of a purely chemical motor. In addition, there are compliance devices such as spring-like proteins called fibronectin [9] and vorticellids [10] and synthetic contractile plant polymers [11].

Application of kinematics is a relatively very new idea in molecular simulations. However, efforts to describe 3-D molecular conformations have been made for the past three decades. There has been work on problems like molecular docking [12], protein folding, receptor-ligand binding [13], alpha-helices packing [14, 15] and applications in drug design [16]. There have also been efforts to generate algorithms to perform conformational search – i.e. search for feasible (low energy) conformations [17-21] and derivation of molecular conformations [22]. Efficient maintenance of molecular conformations can greatly impact the performance of conformational search procedures, energy minimization procedures and all computations that involve large molecules and require frequent recalculation of conformations.

III. The VPL Motor

In this project, we are focusing on the mechanical properties of viral proteins to change their 3D conformation depending on the pH level of environment. Thus, a new linear biomolecular actuator type is obtained that we call: Viral Protein Linear (VPL) motor.

In the first stages of this project, computational and experimental studies are performed using the Influenza virus protein Hemagglutinin (HA) as the basis for forming a VPL motor. The reason for making this peptide selection, is that, based on current literature, this peptide seems to be able to perform repeatable motion controlled by variation of the pH.

The X-ray crystallographic structure of bromelain-released soluble ectodomain of Influenza envelope glycoprotein hemagglutinin (BHA) was solved in 1981 [23]. BHA and pure HA were shown to undergo similar pH-dependant conformational changes which lead to membrane fusion [24]. HA consists of two polypeptide chain subunits (HA1 and HA2) linked by a disulfide bond. HA1 contains sialic acid binding sites, which respond to the cell surface receptors of the target cells and hence help the virus to recognize a cell [25]. Out of the various theories proposed to explain the process of membrane fusion, the spring loaded conformational change theory [26] is the most widely accepted. According to this model, there is a specific region (sequence) in HA2 which tends to form a coiled coil. In the original X-ray structure of native HA, this region is simply a random loop. It further states that a 36 amino-acid residue region, upon activation, makes a dramatic conformational change from a loop to a triple stranded extended coiled coil along with some residues of a short α-helix that precedes it. This process relocates the hydrophobic fusion peptide (and the N-terminal of the peptide) by about 10 nm. In a sense of bio mimicking, we are engineering a peptide identical to the 36-residue long peptide mentioned above, which we call loop36. Cutting out the loop36 from the VPL motor, we obtain a peptide that has a closed length of about 4 nm and an extended length of about 6 nm, giving it an extension by two thirds of its length. Once characterized, the peptide will be subjected to conditions similar to what a virus experiences in the proximity of a cell, that is, a reduced pH. The resulting conformational change can be monitored by fluorescence tagging techniques and the forces can be measured using Atomic Force Microscope.

Figures 2a and 2b show a schematic of the VPL motor supporting a moving platform. The motor is shown in its initial, "contracted" phase that corresponds to the virus' native state (Figure 2a) and at its extended, fusogenic state (Figure 2b).

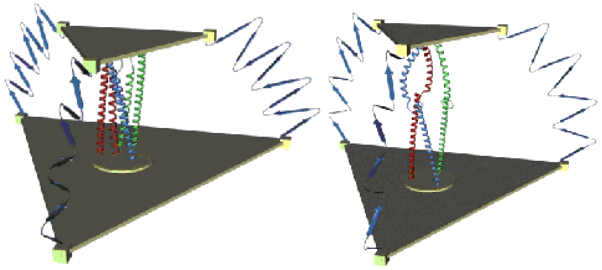

(a) (b)

Fig. 2 (a) Three titin fibers can be used as passive spring elements to join two platforms and form a single degree of freedom parallel platform that is actuated by a viral protein linear (VPL) actuator (center). (b) The VPL actuator has stretched out and this results in the upward linear motion of the platform. The three-titin fibers are also stretched out.

IV. Molecular Dynamics

To predict the dynamic performance of the proposed VPL motors (i.e. energy and force calculation) we are performing Molecular Dynamics (MD) Simulations that are based on the calculation of the free energy that is released during the transition from native to fusogenic state. We used the MD software called CHARMm (Chemistry at Harvard Molecular Mechanics) [27]. In MD, the feasibility of a particular conformation of the biomolecule in question is dictated by the energy constraints. Hence, a transition from one given state to another must be energetically favorable, unless there is an external impetus that helps the molecule overcome the energy barrier. When a macromolecule changes conformation, the interactions of its individual atoms with each other - as well as with the solvent - compose a very complex force system.

Targeted Molecular Dynamics (TMD) is a toolbox of CHARMm that is used for approximate modeling of processes spanning long time-scales and relatively large displacements [28]. Because the distance to be traveled by the N-terminal of the viral protein is relatively very large, we cannot let the protein unfold by itself. Instead of 'unfolding' we want it to undergo a large conformational change and 'open' up. To achieve this, the macromolecule will be 'forced' towards a final configuration 'F' from an initial configuration 'I' by applying constraints. The constraint is in the form of a bias in the force field. If we define the 3N position coordinates corresponding to N atoms in the molecule as

$$\mathbf{X} = \left(X_1, X_2, ..., X_{3N}\right)^T \tag{1}$$

where 3N are the Cartesian coordinates of the position vectors $\mathbf{r_1}, \mathbf{r_2}, ..., \mathbf{r_N}$ of each individual atom, then for each configuration x, its distance, ρ, to the target configuration 'F' is defines as:

$$\rho = \left|\mathbf{x} - \mathbf{x_F}\right| = \left[\sum \left(x_{Ii} - x_{Fi}\right)\right]^2 \tag{2}$$

The distance ρ is a purely geometric control parameter here, which will be used to force the macromolecule to undergo the desired transformation. The constraint applied for this is equal to:

$$f(\mathbf{x}) = \left|\mathbf{x} - \mathbf{x}_\mathbf{F}\right|^2 - \rho^2 \quad (3)$$

This results in an additional constraint force:

$$\mathbf{F}_\mathbf{c} = \lambda \frac{df}{dx} = 2\lambda\left[\mathbf{x} - \mathbf{x}_\mathbf{F}\right] \quad (4)$$

where λ is the Lagrange parameter.

The TMD algorithm steps are:

1) Set $\rho = \rho_0 = |\mathbf{x}_I - \mathbf{x}_F|$, where I is the initial and F is the final conformation.
2) Choose initial coordinates $x_i(o) = x_{Ii}$ and appropriate initial velocities.
3) Solve, numerically, the equations of motion with the additional constraint force $\mathbf{F}_c$.
4) After each time step Δt, diminish ρ by $\Delta\rho = (\rho_0 - \rho_f)\,\Delta t/t_s$, where t_s is the total simulation time.

At the end of the simulation, the final distance ρ_f is reached. In this way, a monotonous decrease of ρ forces the system to find a pathway from x_I to a final configuration x_F.

In this project, the two known states are the native and the fusogenic states of the 36-residue peptide of HA. The structural data on these two states was obtained from Protein Data Bank (PDB) [29]. These PDB files contain the precise molecular make up of the proteins, including the size, shape, angle between bonds, and a variety of other aspects. We used the PDB entries 1HGF and 1HTM respectively, as sources for initial and final states of the peptide.

In a representative simulation, the "open" structure was generated arbitrarily by forcing the structure away from the native conformation with constrained high-temperature molecular dynamics. After a short equilibration, these two "closed" and "open" structures are then used as reference end-point states to study the transformation between the open and closed conformations. The transformation is enforced through a root mean square difference (RMSD) harmonic constraint in conjunction with molecular dynamics simulations. Both the forward (closed to open) and the reverse (open to closed) transformations are carried out. The RMSD between the two end-point structures is about 9Å, therefore the transformation is carried out in 91 intermediate steps or windows with a 0.1 Å RMSD spacing between each intermediate window. At each intermediate window, the structure is constrained to be at the required RMSD value away from the starting structure, it is minimized using 100 steps of Steepest Descent minimization, and then equilibrated with 0.5 picoseconds of Langevin dynamics with a friction coefficient of 25 ps on the non-hydrogen atoms. The harmonic RMSD constraint is mass-weighted and has a force constant of 500 kcal/mol/ Å^2 applied only to the non-hydrogen atoms. The decision to calculate the RMSD only for non-hydrogen atoms is usually done by convention since the conformation of the protein is more directly dependent on the heavy atoms than on the hydrogen atoms. Spontaneous transformation between the two conformations using unconstrained molecular dynamics may occur in the microsecond timescale. In the present case, however, the transformation is speeded up by using the artificial RMSD constraint such that a conformation close to the final state is approached successfully. Figure 3 shows the RMSD values of the structures at the end of each intermediate window from both the native closed (non-fusogenic) and the open (fusogenic) conformations. The two curves shown correspond to the forward and reverse transformations, respectively, and the difference between the two curves is due to hysteresis. A small RMSD value on the x-axis indicates that the structure is close to the native conformation while a small RMSD value on the y-axis indicates that the structure is close to the closed conformation. In both curves, it can be seen that structures close to the end-point states (RMSD < 1 Å) are obtained. Increase in the amount of sampling for each window and decrease in the value of the force constant used in this transformation can lead to a progressively better description of the transformation. The energy plot using solvation function EEF1 [30] is shown in Figure 4 and the simulation snapshots for the intial and final states are shown in Figures 5 and 6.

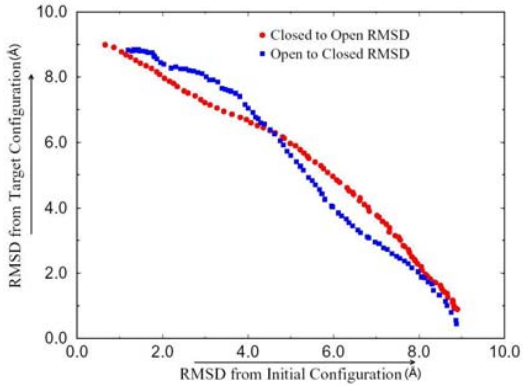

Fig. 3 The non-hydrogen RMSD values of the structures at the end of each window in the constrained molecular dynamics transformation between the closed (native, non-fusogenic) and the open (fusogenic) states of the 36 amino acid peptide test system. The RMSD values (in Å) in comparison to the closed state are on the x-axis, those in comparison to the open state are on the y-axis. The two curves correspond to the forward (closed to open) and the reverse (open to closed) transformations, respectively.

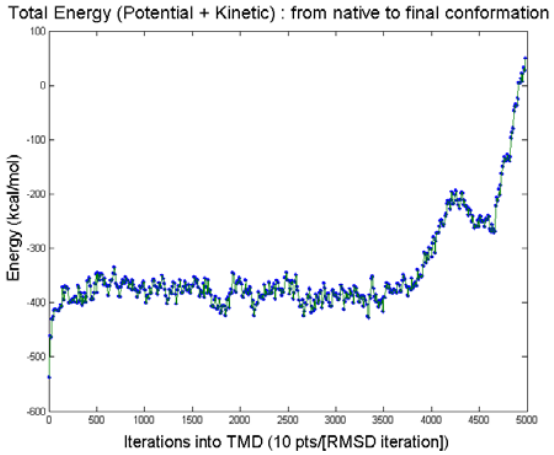

Fig. 4: Energy variation for LOOP-36 peptide with salvation model EEF1.

By using TMD we have been able to prove that the final state of the VPL shown in Figure 6 is feasible, and it is the result of the action of the applied potentials. However, from the energy graph in Figure 4 we learn that even though the 36-

residue long protein is forced to undergo a conformational change, it would require an energy jump to overcome the barrier that appears at approximately 4000 iterations. Unless an external force induces that jump, the protein would not go naturally to that state. TMD works well in the first stages of the change in structure, since the protein does not require much provocation to transform into an intermediate conformation. Only after 4000 iterations more energy is required. In fact, the opening of the helical region followed by the adjustment of the remaining loop into an α-helical form is what requires more energy. This process occurs solely due to the pH drop in the natural setting of VPL since it is the rest of the large protein attached to the ends of this loop-36 that affects its behavior.

A more realistic environment of the VPL requires the inclusion of the effect of pH on the protein. For this, 10 titrable amino acids (Glutamic Acid - GLU, Aspartic Acid - ASP, and Histidine - HIS) were chosen out of the VPL sequence to be protonated. New topology files were used to replace them with their protonated counterparts, and the effect on the structure was observed.. So far there has been very little observable effect; however new efforts are underway to simulate water molecules explicitly around the protein using stochastic and periodic boundary conditions. We are also considering a model that takes into account the real-time effect of pH on the ionic stability of the protein so as to affect a conformation change.

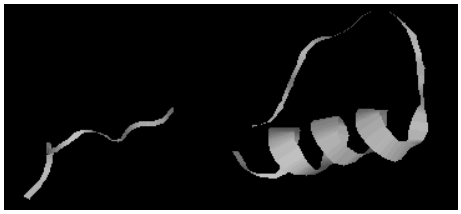

Fig. 5 Ribbon drawing of the closed conformation of 36-residue peptide as obtained from PDB entry 1HGF.

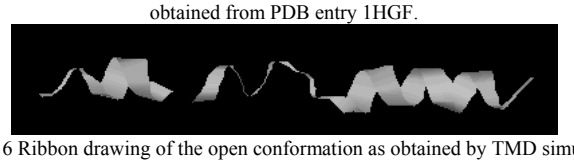

Fig. 6 Ribbon drawing of the open conformation as obtained by TMD simulations. There is a noticeable increase in alpha-helical content and the peptide opens.

V. MOLECULAR KINEMATICS

Molecular kinematic simulations are being developed to study the geometric properties and conformational space of the VPL motors. The kinematic analysis is based on the development of direct and inverse kinematic models and their use towards the workpspace analysis of the VPL motors. In this section we present the derivation of the direct and inverse kinematic modules that have been incorporated into a MATLAB toolbox called BioKineLab that has been developed in our laboratory to study protein kinematics.

Proteins are macromolecules that are made up from 20 different types of amino acids, also called residues. For kinematics purpose we consider these residues to be connected in a serial manner to create a serial manipulator. The "back bone" of the chain is a repeat of the Nitrogen - Alpha Carbon – Carbon (–N-Cα-C-) sequence. To the Cα atom is also attached a side-chain (R) which is different for each residue. These side-chains are passive 3-D structures with no revolute joints. Hydrogen atoms are neglected because of their small size and weight. The C-N bond joins two amino acid residues and has a partial double bond character and is thus non- rotatable. There are however two bonds which are free to rotate. These are the N-Cα and Cα-C bonds and the rotation angles around them are known as *phi* (φ) and *psi* (ψ) respectively. The value of these angles determines the 3-D structure of the protein and makes it perform its function. Therefore, a protein is considered to be a serial linkage with K+1 solid links connected by K revolute joints (Figure 7). In case of loop36, K takes the value 72. In most kinematic studies, bond lengths and bond angles are considered constant, while the torsional angles (φ and ψ) are allowed to change [18].

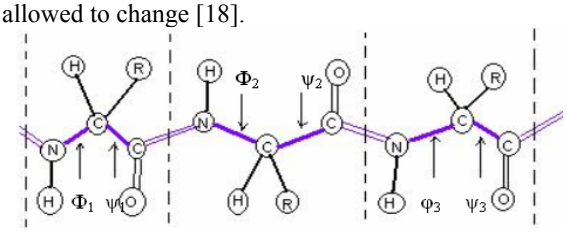

Fig. 7: Rotational degrees of freedom along a residue chain. Adjacent residues are separated by dashed lines; side chains are denoted by R, purple line represents the back-bone.

A. Direct Kinematics

The direct kinematics problem calculates the VPL motor's final configuration when an initial configuration is given, all constant parameters of the chain are specified and a specific set of rotations for the torsional angles is defined. Frames are affixed at each backbone atom (Figure 8). Let b_i be a bond between atoms Q_i and Q_{i-1}. A local frame $F_{i-1} = \{Q_{i-1}; \mathbf{x}_{i-1}, \mathbf{y}_{i-1}, \mathbf{z}_{i-1}\}$ is attached at bond b_{i-1} as follows: $\mathbf{z}_{i-1}$ has the direction of bond b_{i-1}; $\mathbf{x}_{i-1}$ is perpendicular to both b_{i-1} and b_i; and $\mathbf{y}_{i-1}$ is perpendicular to both $\mathbf{x}_{i-1}$ and $\mathbf{z}_{i-1}$ (Figure 8). Similarly, a local frame $F_i = \{Q_i; \mathbf{x}_i, \mathbf{y}_i, \mathbf{z}_i\}$ is attached to bond b_i [23]. The Protein Denavit-Hartenberg (PDH) parameters are defined to facilitate the geometric representation of one frame to another [31] as follows: a_i is the distance from $\mathbf{z}_{i-1}$ to $\mathbf{z}_i$ measured along $\mathbf{x}_{i-1}$; α_i is the angle between $\mathbf{z}_{i-1}$ and $\mathbf{z}_i$ measured about $\mathbf{x}_{i-1}$; b_i is the distance from $\mathbf{x}_{i-1}$ to $\mathbf{x}_i$ measured along $\mathbf{z}_i$; and θ_i is the angle between $\mathbf{x}_{i-1}$ and $\mathbf{x}_i$ measured about $\mathbf{z}_i$. The coordinates of the origin and of the unit vectors of frame F_i with respect to frame F_{i-1} are represented using the following 4 x 4 homogeneous transformation matrix [32] where $c\theta_i$ is the $\cos(\theta_i)$, $s\theta_i$ is the $\sin(\theta_i)$, $c\alpha_{i-1}$ is the $\cos(\alpha_{i-1})$, $s\alpha_{i-1}$ is the $\sin(\alpha_{i-1})$, l_i is the length of the bond b_i, θ_i is the torsional angle of b_i, and α_{i-1} is the bond angle between b_{i-1} and b_i:

$$R_i = \begin{bmatrix} c\theta_i & -s\theta_i & 0 & 0 \\ s\theta_i c\alpha_{i-1} & c\theta_i - c\alpha_{i-1} & -s\alpha_{i-1} & l_i s\alpha_{i-1} \\ s\theta_i s\alpha_{i-1} & c\theta_i s\alpha_{i-1} & -c\alpha_{i-1} & l_i c\alpha_{i-1} \\ 0 & 0 & 0 & 1 \end{bmatrix} \quad (5)$$

If an atom Q_i is connected to the root atom Q_0 by a sequence of bonds $b_i, \ldots, b_1$, then the coordinates of Q_i with respect to frame F_0 are:

$$\begin{pmatrix} x' & y' & z' & 1 \end{pmatrix}^T = R_1 \cdots R_i \bullet \begin{pmatrix} 0 & 0 & 0 & 1 \end{pmatrix}^T \quad (6)$$

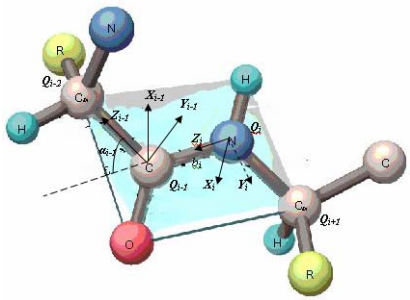

Fig. 8 Frames F_{i-1} and F_i are attached to parent atom Q_{i-1} and Q_i and bond rotation angle is α_{i-1}.

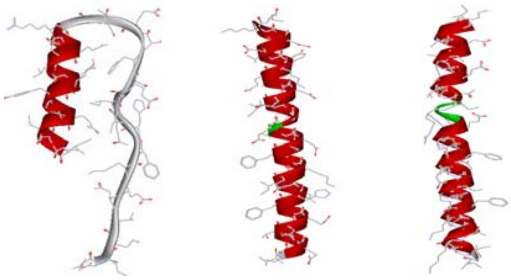

(a) (b) (c)

FIGURE 9: (a) loop36 protein in the native state, (b) open state generated by NMR experiments which is similar to that generated by MD, computation time for MD is about 2 hours, (c) open state generated by molecular kinematics, computation time is less than 40 seconds.

In a similar way, the position of any atom on a side chain can be calculated with the respect to the root frame F_0.

A representative result of the direct kinematics module of the BioKineLab Toolbox is shown in Figure 9**.** The results are obtained by running direct kinematics simulations on the native state of loop36 as shown in Fig. 9a. The final state of the same protein obtained from NMR (Nuclear Magnetic Resonance) experiments is shown in Fig. 9b. Note that the random coil portion has turned into an α-helix after transformation giving us a linear motion of the end-effector. The goal was to achieve the final loop36 conformation using direct kinematics techniques. For this the torsional angles corresponding to the final state were determined using the Accerlys Viewer ActiveX software. These angles along with the initial state of loop36 were given as an input to the direct kinematics module of BioKineLab. Figure 9c shows the final structure generated by BioKineLab which gives a very good approximation of the actual output and clearly shows the relevance of using molecular kinematics for predicting and generating protein conformations.

B. Inverse Kinematics

The inverse kinematics problem calculates the VPL motor's torsional angles given an initial and final conformation and when all constant parameters of the chain are specified. A modified version of the Cyclic Coordinate Descent (CCD) method is used here. The CCD algorithm was initially developed for the inverse kinematics applications in robotics [33]. For the inverse kinematics of protein chains, the torsional angles must be adjusted to move the C-terminal (end-effector) to a given desired position. The CCD method involves adjusting one torsional angle at a time to minimize the sum of the squared distances between the current and the desired end-effector positions. Hence, at each step in the CCD method the original *n*-dimensional minimization problem is reduced to a simple one-dimensional problem (Figure 10). The algorithm proceeds iteratively through all of the adjustable torsional angles from the C-terminal to the base N-terminal.

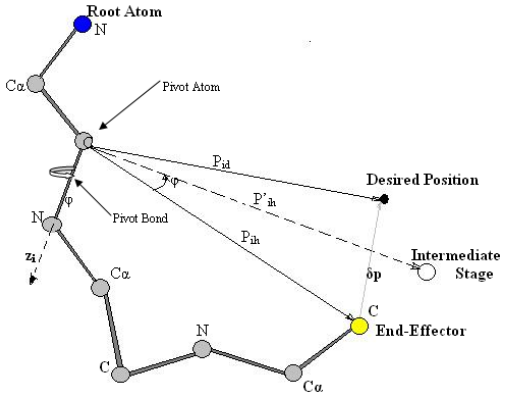

Fig. 10: One step of the CCD method.

At any given CCD step the bond around which the rotation is being performed is called the pivot bond and its preceding atom is called the pivot atom. The torsional angle corresponding to the pivot bond is to be determined. Figure 11 is the ball and stick model of a segment of the protein before and after the inverse kinematics simulation. Side chains are not shown for clarity. Table 1 shows the inverse kinematics results of the CCD simulations.

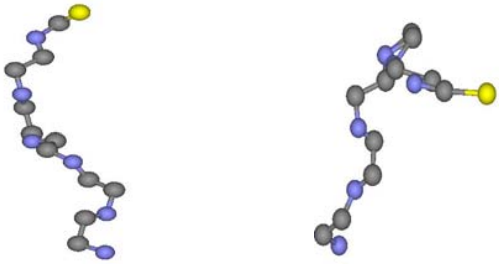

Fig. 11: Initial conformation of the protein (left) and one of the solutions found by CCD simulations (right).

TABLE 1: RESULTS OF INVERSE KINEMATICS WITH LOOP36

	X (Å)	Y (Å)	Z (Å)
End-effector Initial Position	23.3	81.7	228.0
Desired Position	26.0	75.0	224.0
Position Reached	26.0	74.8	223.9
Error (Å)	0.1566		
Number of Iterations	31		

VI. CONCLUSIONS

In this paper the concept of the Viral Protein Linear nanomotor was presented. Dynamic and kinematic analysis methods were described to calculate important properties of the motor. Preliminary results from the application of these computational methods in the VPL motor were shown. The dynamic analysis, though slower, attempts a more realistic representation of the system. Each intermediate conformation is energy minimized to make sure that it is stable and feasible. Targeted molecular dynamics studies show that a large impetus is needed to make the protein undergo the desired conformational change unless there are other environmental factors

present due to the presence of the remaining part of the protein not taken into account in this study. It however assures of the stability of the two end states of the system predicted by the kinematic analysis and experimental observations. Kinematics analysis can suggest the geometric paths that could be followed by the protein during the transition, while dynamics will narrow down the possibilities by pointing at the only energetically feasible paths. A combination of the two approaches – kinematics to give quick initial results and dynamics to corroborate and select the feasible solutions – can prove to be an indispensable tool in bio-nano-robotics.

The future of bio-nano machines is bright. We are at the dawn of a new era in which many disciplines will merge including robotics, mechanical, chemical and biomedical engineering, chemistry, biology, physics and mathematics so that fully functional systems will be developed. However, there remain many hurdles to overcome to reach this goal. Developing a complete database of different biomolecular machine components, the ability to interface or assemble different machine components and the development of accurate models are some of the challenges to be faced in the near future. The problems involved in controlling and coordinating several bionano machines will come next.

ACKNOWLEDGMENTS

This work was supported by the National Science Foundation (DMI-0228103 and DMI–0303950). Any opinions, findings, conclusions or recommendations expressed in this publication are those of the authors and do not necessarily reflect the views of the National Science Foundation.

REFERENCES

[1] Block S.M., 1998, "Kinesin, What Gives?" *Cell*, **93**, 5–8.

[2] Schnitzer M.J. and Block S.M., 1997, "Kinesin Hydrolyses One ATP per 8-nm Step", *Nature*, **388**, 386-390.

[3] Wang M.D., Schnitzer M.J., Yin H., Landick R., Gelles J., Block S. M., 1998, "Force and Velocity Measured for Single Molecules of RNA Polymerase", *Science*, **282**, 902-907.

[4] Kitamura K., Tokunaga M., Iwane A.H., Yanagida T., 1999, "A Single Myosin Head Moves along an Actin Filament with Regular Steps of ~5.3nm", *Nature*, **397**, 129.

[5] Shingyoji C., Higuchi H., Yoshimura M., Katayama E. and Yanagida T., 1998, "Dynein arms are oscillating force generators", *Nature*, **393**, 711-714.

[6] Montemagno C.D., and Bachand G.D., 1999, "Constructing Nanomechanical Devices Powered by Biomolecular Motors", *Nanotechnology*, **10**, 225-331.

[7] Berg H.C., 1974, "Dynamic Properties of Bacterial Flagellar Motors", *Nature*, **249**, 77-79.

[8] Schalley C.A., Beizai K. and Vogtle F.K., 2001, "On the Way to Rotaxane-Based Molecular Motors: Studies in Molecular Mobility and Topological Chirality", *Accounts of Chemical Research*, **34**, 465-476.

[9] Erickson, H.P., 1997, "Stretching Single Protein Molecules: Titin is a Weird spring", *Science*, **276**,1090-1092.

[10] Mahadevan L. and Matsudaira P., 2000, "Motility Powered by Supramolecular Springs and Ratchets", *Science*, **288**, 95-99.

[11] Knoblauch M, Noll GA, Muller T, Prufer D, Schneider-Huther I, et al. 2003. ATP-independent contractile proteins from plants. *Nature Materials,* **2**: 600-603.

[12] Teodoro M., Phillips G. N. Jr., and Kavraki L. E., "Molecular Docking: A Problem with Thousands of Degrees of Freedom", *Proc. of the 2001 IEEE International Conference on Robotics and Automation (ICRA 2001)*, pp. 960–966, 2001.

[13] Finn P. W., Halperin D., Kavraki L. E., Latombe J.-C., Motwani R., Shelton C., and Venkat S., "Geometric Manipulation of Flexible Ligands", *LNCS Series Applied Computational Geometry - Towards Geometric Engineering*, pp. 67–78.

[14] Moon K. Kim, Gregory S. Chirikjian and Robert L. Jernigan, "Elastic Models of Conformational Transitions in Macromolecules", *Journal of Molecular Graphics and Modeling*, 21:151-160, 2002.

[15] Moon K. Kim, Robert L. Jernigan and Gregory S. Chirikjian, "Efficient Generation of Feasible Pathways for Protein Conformational Transitions", *Biophysical Journal*, 83, 2002.

[16] Finn P. W. and Kavraki L. E., "Computational Approaches to Drug Design", *Algorithmica*, 347–371, 1999.

[17] LaValle S. M., Finn P. W., Kavraki L. E., and Latombe J.-C., "A Randomized Kinematics-based Approach to Pharmacophore-Constrained Conformational Search and Database Screening", *Journal of Computational Chemistry*, 21(9), 731–747, 2000.

[18] Gardiner E. J., Willett P. and Artymiuk P. J., "Graph-theoretic techniques for macromolecular docking", *Journal of Chemical Information and Computer Sciences*, 40, 273-279, 2000.

[19] Jones G., Willett P., Glen R. C., Leach A. R., Taylor R., 1999, "Further development of a genetic algorithm for ligand docking and its application to screening combinatorial libraries", *ACS Symposium Series (Rational Drug Design: Novel Methodology and Practical Applications)*, 719, 271-291.

[20] Lipton M., and Still W., "The Multiple Minimum Problem in Molecular Modeling. Tree Searching Internal Coordinate Conformational Space" *Journal of Computational Chemistry*, 1998, 9, pp 343-355.

[21] Smellie A., Kahn S. D., and Teig S. L., 1995, "Analysis of Conformational Coverage - 1. Validation and Estimation of Coverage", *Journal of Chemical Information and Computer Science*, 35, 285-294.

[22] Zhang M., Kavaraki L., 2002, "A new method for fast and accurate derivation of molecular conformations", *Journal of Chemical Information and Computer Science*, 42, 64-70.

[23] Wilson I.A., Skehel J.J., Wiley D.C., 1981, "Structure of the haemagglutinin membrane glycoprotein of influenza virus at 3 A resolution", *Nature*, **289**, 377-373.

[24] Skehel J.J., Bayley P.M., Brown E.B., Martin S.R., Waterfield M.D., White J.M., Wilson I.A., Wiley D.C., 1982, "Changes in the conformation of influenza virus hemagglutinin at the pH optimum of virus-mediated membrane fusion", *PNAS USA*, **79**, 968-972.

[25] Sauter N.K, Bednarski M.D., Wurzburg B.A., Hanson J.E., Whitesides G.M., Skehel J.J., and Wiley, D.C., 1989, "Hemagglutinins from Two Influenza Virus Variants Bind to Sialic Acid Derivatives with Millimolar Dissociation Constants: A 500 MHz Proton Nuclear Magnetic Resonance Study", *Biochemistry,* **28**, 8388-8396.

[26] Carr C. M. and Kim P., 1993, "A Spring-Loaded Mechanism for the Conformational Change of Influenza Hemagglutinin," *Cell*, **73**, 823-832.

[27] Brooks R., Bruccoleri R.E., Olafson B.D., States D.J., Swaminathan S., and Karplus M., 1983, "CHARMM: A Program for Macromolecular Energy, Minimization, and Dynamics Calculations", *Journal of Computational Chemistry* **4**, 187-217.

[28] Schlitter J., 1994, "Targeted Molecular Dynamics: A New Approach for Searching Pathways of Conformational Transitions", *Journal of Molecular Graphics*, **12**,84-89.

[29] Berman H.M, Westbrook J., Feng Z., Gilliland G., Bhat T.N., Weissig H., Shindyalov I.N., and Bourne P.E., 2000, "The Protein Data Bank," *Nucleic Acid Research,* **28**, 235-242.

[30] Lazaridis T., and Karplus M., 1999, "Effective Energy Function for Proteins in Solution," *Proteins: Structure, Function and Genetics*, **35**,133-152.

[31] Denavit J., and Hartenberg S., 1955, "A Kinematic Notation for Lower Pair Mechanisms Based on Matrices", *ASME Journal of Applied Mechanics*, pp 215-221.

[32] McCarthy J., "Geometric Design of Linkages", *Springer Publications NY*, 2000.

[33] Wang L.C.T, Chen C.C, "A Combined Optimization Method for Solving the Inverse Kinematics Problem of Mechanical Manipulators", *IEEE Transactions on Robotics and Automation*, 7(4):489-499, 1991.